Structural, mechanical and electronic properties of 3d transition metal nitrides in cubic zincblende, rocksalt and cesium chloride structures: a first-principles investigation

2014 J. Phys.: Condens. Matter 26 025404

(http://iopscience.iop.org/0953-8984/26/2/025404)

IOP Publishing Journal of Physics: Condensed Matter
J. Phys.: Condens. Matter **26** (2014) 025404 (10pp) doi:10.1088/0953-8984/26/2/025404

Structural, mechanical and electronic properties of 3d transition metal nitrides in cubic zincblende, rocksalt and cesium chloride structures: a first-principles investigation

Z T Y Liu[1], X Zhou[2], S V Khare[1] and D Gall[3]

[1] Department of Physics and Astronomy, The University of Toledo, 2801 West Bancroft Street, Toledo, OH 43606, USA
[2] Department of Chemistry and Biochemistry, The University of Toledo, 2801 West Bancroft Street, Toledo, OH 43606, USA
[3] Department of Materials Science and Engineering, Rensselaer Polytechnic Institute, 110 8th Street, Troy, NY 12180, USA

E-mail: sanjay.khare@utoledo.edu

Received 5 August 2013, in final form 14 October 2013
Published 5 December 2013

Abstract

We report systematic results from *ab initio* calculations with density functional theory on three cubic structures, zincblende (zb), rocksalt (rs) and cesium chloride (cc), of the ten 3d transition metal nitrides. We computed lattice constants, elastic constants, their derived moduli and ratios that characterize mechanical properties. Experimental measurements exist in the literature of lattice constants for rs-ScN, rs-TiN and rs-VN and of elastic constants for rs-TiN and rs-VN, all of which are in good agreement with our computational results. Similarly, computed Vickers hardness (H_V) values for rs-TiN and rs-VN are consistent with earlier experimental results. Several trends were observed in our rich data set of 30 compounds. All nitrides, except for zb-CrN, rs-MnN, rs-FeN, cc-ScN, cc-CrN, cc-NiN and cc-ZnN, were found to be mechanically stable. A clear correlation in the atomic density with the bulk modulus (B) was observed with maximum values of B around FeN, MnN and CrN. The shear modulus, Young's modulus, H_V and indicators of brittleness showed similar trends and all showed maxima for cc-VN. The calculated value of H_V for cc-VN was about 30 GPa, while the next highest values were for rs-ScN and rs-TiN, about 24 GPa. A relation ($H_V \propto \theta_D^2$) between H_V and Debye temperature (θ_D) was investigated and verified for each structure type. A tendency for anti-correlation of the elastic constant C_{44}, which strongly influences stability and hardness, with the number of electronic states around the Fermi energy was observed.

(Some figures may appear in colour only in the online journal)

1. Introduction

In the quest for super-hard materials widely used in cutting and coating industries, attention has been drawn to transition metal nitrides (TMNs). Due to the large number of valence electrons in transition metals, small covalent radii of nitrogen and other determining factors, some TMNs exhibit high incompressibility, high hardness and a high melting point, making them compelling candidates for industrial use. These properties have led to significant fundamental work focused on TMNs [1–8].

Recently, activity in TMNs received new impetus from the experimental discovery of osmium nitride (OsN_2) [9, 10], iridium nitride [10, 11], platinum nitride [11, 12] and other

novel phases [13–15]. There are many theoretical studies investigating the elastic and mechanical properties of 4d and 5d transition metal nitrides, including ones of specific compositions and structures that demonstrate extraordinary properties. These include the studies on technetium nitrides by Liang *et al* [16], osmium nitride (OsN_4) by Zhao *et al* [17] and platinum nitrides by Patil *et al* [18]. More studies involving a systematic search throughout the transition metal region of the periodic table in many different structures have provided thorough data and organized knowledge to better explain and predict material properties. Among them, Zhao *et al* studied the structural, elastic and electronic properties of rocksalt-, NiAs- and WC-structured 4d transition metal mono-nitrides [19], and more structures of 5d transition metal mono-nitrides [20]. Patil *et al* [21] also investigated the 5d transition metal nitrides systematically, including zincblende, rocksalt, fluorite and pyrite structures, not limited to 1:1 stoichiometry. Chen and Jiang [22] studied both 4d and 5d metal nitrides in zincblende and rocksalt structures and their work is rich in figures of density of states and band structures. For 3d transition metal nitrides, the composition- and structure-specific theoretical studies of elastic properties were mostly on early transition metal elements such as Sc, Ti, V and Cr, and solely on rocksalt structures, by Holec *et al* [23], Brik and Ma [24] and Zaoui *et al* [25]. On the other hand, Eck *et al* [26] did systematic calculations on the structural, electronic and magnetic properties of nitrides in zincblende and rocksalt structures. Häglund *et al* [27] evaluated band structure and cohesive energies of phases in rocksalt structure. However, neither of these two papers reported elastic constants and mechanical parameters, which are the main interest in this work. Hence, we have conducted our present investigation, with first-principles computations, to obtain the lattice constants, elastic constants, derived mechanical properties and their relation to electronic properties of all 3d TMNs in three different 1:1 cubic structures, namely zincblende (zb), rocksalt (rs) and cesium chloride (cc), which are either observed experimentally or are plausible structures, but certainly not the only possibilities. We selected these three structures because the rs structure is widely observed for TiN and VN [28–33] and the zb structure is similar to diamond, fluorite and pyrite structures, which may lead to super-hardness [12, 18]. The cc structure is simple and has been studied theoretically for 5d TMNs and is expected for some nitrides at high pressure [20, 34]. As has been commented earlier [35], there are several isomorphs of transition metal carbides that may exist for the corresponding nitrides. The present work does not address all such structures, though they could exist and may be important. Thus other structures including those with other metal to nitrogen ratios and those in other crystallographic systems [20, 34–38], such as wurtzite, nickel arsenide (NiAs) and tungsten carbide (α-WC), are beyond the scope of this work.

Our computed values for lattice constant, elastic constants and hardness agree well with other calculations and the results of some experimentally explored phases, such as rs-TiN and rs-VN. The predictive nature of *ab initio* computations for elastic and mechanical properties makes our materials by design approach valuable. It is likely to speed experimental discovery of new materials by eliminating effort on unstable phases and focusing it on desirable elements and structures.

2. Computational method

We performed *ab initio* total energy calculations with density functional theory (DFT) [39] using the suit of codes of the Vienna *ab initio* simulation package (VASP) [40–42]. Ultra-soft Vanderbilt pseudo-potentials (US-PP) [43] as supplied by Kresse and Hafner [44], with local density approximation (LDA) [45] and PW91 general gradient approximation (GGA) [46] were both used. It is known that LDA underestimates the lattice constant and overestimates the elastic constants and cohesive energy, while PW91 GGA does the opposite for the lattice constant and elastic constants by a smaller amount and yields more accurate values of cohesive energy [47, 48]. Similar trends have been observed by several other authors [37, 49–54]. Hence, we report computational results of the lattice constant, elastic constants and the total energy obtained from both approximations, and the rest of the calculations using GGA in the present work. We chose the kinetic energy cutoff value to the plane-wave basis set of the single-particle wavefunction expansion to be 450 eV for all tested nitrides, and the high precision mode in VASP, providing dense FFT grids. The electronic self-consistent loops were set to converge below 10^{-4} eV/atom. For k-points we used a 12 × 12 × 12 Monkhorst–Pack mesh [55] for all zb and rs structures, and a 22 × 22 × 22 gamma point centered mesh for the cc structure. Convergence tests revealed the need for the denser mesh since the volumes of cc-structured primitive cells are often half the volumes of zb- and rs-structured ones. Tests using a higher energy cutoff value and a denser k-point mesh suggested that total energy convergence below ±1 meV was reached.

Total energy was directly calculated from the computational output data of VASP. We implemented $E_{\mathrm{coh}} = (E_{\mathrm{M}} + E_{\mathrm{N}} - E_{\mathrm{MN}})/2$ to calculate the cohesive energy per atom, where E_{MN}, E_{M} and E_{N} are total energies of the nitride, single transition metal atom and single nitrogen atom, respectively.

Lattice constants (a) were varied in a range of 1 Å bracketing the value corresponding to the lowest total energy. The data were fit to the Murnaghan equation of state [56, 57] to get an initial estimate of the equilibrium lattice constant. Further refinement by varying lattice constants in steps of 0.01 Å over a range of 0.06 Å near the minimum achieved in the previous step was then performed. These refined results were fitted to a second order polynomial to obtain the precise value. The bulk modulus was also calculated in this step for a consistency check for comparison with the one achieved from the elastic constants later.

To obtain the three independent single crystal elastic constants for cubic systems, C_{11}, C_{12} and C_{44}, we applied three sets of strains to our primitive cells and fitted the resultant total energy to second order polynomials. The polynomial coefficients were used to solve three linear equations to determine the elastic constants, primarily as

Table 1. Lattice constant (a), elastic constants (C_{11}, C_{12}, C_{44}), mechanical stability and cohesive energy per atom (E_{coh}) of the nitrides (MN) of 3d transition metals (M) in the zincblende structure. Stable phases are denoted as 'S' and unstable ones as 'U'.

	a (Å)		C_{11} (GPa)		C_{12} (GPa)		C_{44} (GPa)		Mechanical stability		E_{coh} (eV/atom)	
M	LDA	GGA	LDA	GGA	LDA	GGA	LDA	GGA	LDA	GGA	LDA	GGA
Sc	4.840	4.925	186.9	172.4	140.9	124.9	73.8	69.8	S	S	7.05	6.17
Ti	4.529	4.609	322.2	292.2	176.4	154.1	103.1	95.3	S	S	7.78	6.69
V	4.368	4.446	346.8	309.4	229.4	196.5	43.2	42.4	S	S	7.20	5.93
Cr	4.262	4.342	361.7	320.5	258.7	221.8	−77.9	−54.5	U	U	6.08	4.69
Mn	4.188	4.269	372.7	331.4	279.7	235.5	24.0	42.9	S	S	5.95	4.51
Fe	4.160	4.243	379.2	334.6	282.8	234.6	114.2	110.6	S	S	6.52	5.14
Co	4.177	4.265	347.4	297.6	266.0	219.9	71.2	65.3	S	S	6.45	5.35
Ni	4.241	4.336	278.1	232.9	246.2	200.8	49.9	43.5	S	S	5.68	4.55
Cu	4.344	4.452	222.4	183.0	199.9	160.1	41.1	37.7	S	S	4.35	3.34
Zn	4.472	4.588	178.0	144.7	159.4	126.6	47.4	42.6	S	S	3.39	2.50

detailed by Patil *et al* [18]. For relaxation of ions into equilibrium, the conjugate-gradient algorithm was used until a force tolerance of 0.01 eV Å^{-1} was reached for each atom. The strains were chosen to be below 3% to maintain second order polynomial behavior.

With the three independent elastic constants obtained with GGA potentials, we calculated the mechanical properties of the material, including the bulk modulus (B) given by $B = (C_{11}+2C_{12})/3$, the Cauchy pressure (P_C) by $P_C = C_{12}-C_{44}$, the polycrystalline shear modulus in various forms like the Voigt approximation (G_V), the Reuss approximation (G_R) and Hill's arithmetic mean (G) as given by

$$G_V = [(C_{11} - C_{12}) + 3C_{44}]/5, \quad (1)$$

$$G_R = [5(C_{11} - C_{12})C_{44}]/(4C_{44} + 3C_{11} - 3C_{12}), \quad (2)$$

$$G = (G_V + G_R)/2. \quad (3)$$

From these we may further obtain Pugh's ratio (k) as $k = G/B$, Poisson's ratio (ν) as $\nu = (3 - 2k)/[2(3 + k)]$, Young's modulus ($E$) as $E = 9G/(3 + k)$ and the Debye temperature (θ_D) which has a more complex form given in equations (4) and (5):

$$\theta_D = \frac{h}{k_B}\left[\frac{3n}{4\pi}\left(\frac{N_A\rho}{M}\right)\right]^{1/3} v_m,$$

$$\text{where } v_m = \left[\frac{1}{3}\left(\frac{2}{v_t^3} + \frac{1}{v_l^3}\right)\right]^{-1/3}, \quad (4)$$

$$v_t = \left(\frac{G}{\rho}\right)^{1/2} \quad \text{and} \quad v_l = \left(\frac{3B + 4G}{3\rho}\right)^{1/2}. \quad (5)$$

Here h is Planck's constant, k_B is Boltzmann's constant, N_A is Avogadro's number, ρ is the mass density, M is the molecular weight of the primitive cell and n is the number of atoms in the cell for which M is calculated. The transverse, longitudinal and mean sound speeds are v_t and v_l and v_m, respectively.

The electronic density of states, local or projected (LDOS) and total (TDOS) were computed with GGA potentials, using the tetrahedron method with Blöchl corrections [58] for the energy and denser gamma point centered meshes (1.5 times the original divisions).

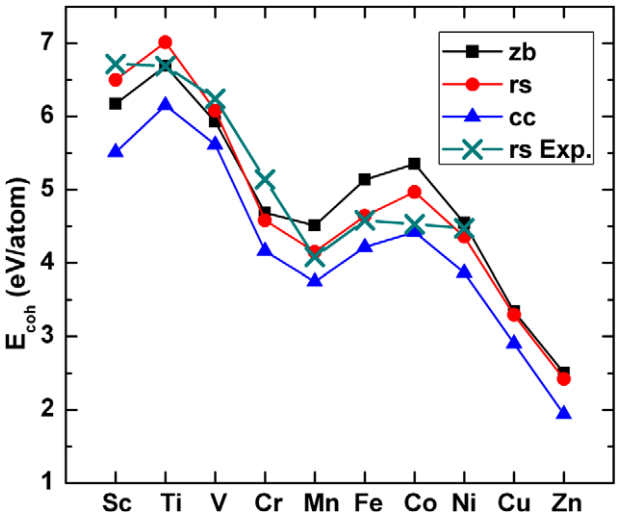

Figure 1. Cohesive energy per atom of the nitrides (MN) versus their corresponding 3d transition metals (M). The three structures are zincblende (zb, black square), rocksalt (rs, red circle) and cesium chloride (cc, blue triangle). Experimental values for the rocksalt structure (green ×) from [27] are also presented.

3. Results and discussion

To assess the relative energetic stability of different phases of the nitrides studied, we give the cohesive energy (E_{coh}) of zb-, rs- and cc-structured nitrides from both approximations in tables 1–3, and plotted values from the GGA in figure 1. Our results are very close to the experimental values taken from Häglund *et al* [27]. From the trend we see that for ScN, TiN and VN, rs is the most stable structure because it has the highest value of E_{coh}, and for others it is zb structure. Nitrides with the cc structure, however, always have the lowest value of E_{coh} compared to rs or zb structures. Therefore the cc structure is the least stable for each element. A similar observation of the relative stability advantage of rs-TiC and rs-VC and its loss of relative stability to other structures starting from CrC in the 3d transition row was also obtained by Hugosson *et al* [35]. They have also commented that these results are expected due to the similarity of the electronic structures in nitrogen and carbon.

Table 2. Lattice constant (a), elastic constants (C_{11}, C_{12}, C_{44}), mechanical stability and cohesive energy per atom (E_{coh}) of the nitrides (MN) of 3d transition metals (M) in rocksalt structure. Stable phases are denoted as 'S' and unstable ones as 'U'.

	a (Å)		C_{11} (GPa)		C_{12} (GPa)		C_{44} (GPa)		Mechanical stability		E_{coh} (eV/atom)	
M	LDA	GGA	LDA	GGA	LDA	GGA	LDA	GGA	LDA	GGA	LDA	GGA
Sc	4.463	4.543	470.1	399.3	99.4	95.9	164.3	157.6	S	S	7.49	6.50
	4.516[a]		390[a]		105[a]		166[a]					
	4.445[b]	4.516[b]	418.72[b]	354.06[b]	101.79[b]	100.20[b]	173.48[b]	170.00[b]				
	4.44[c]											
Ti	4.184	4.258	712.3	603.0	123.2	118.7	171.1	159.6	S	S	8.23	7.01
	4.253[a]		560[a]		135[a]		163[a]					
	4.185[b]	4.250[b]	648.96[b]	534.67[b]	129.01[b]	117.70[b]	193.96[b]	175.42[b]				
	4.241[c]		625[d]		165[d]		163[d]					
			507[e]		96[e]		163[e]					
V	4.057	4.133	751.1	620.5	178.9	166.8	126.6	116.5	S	S	7.46	6.08
	4.127[a]		660[a]		174[a]		118[a]					
	4.057[b]	4.119[b]	763.16[b]	628.70[b]	148.70[b]	144.63[b]	158.27[b]	147.41[b]				
	4.139[c]		533[d]		135[d]		133[d]					
Cr	3.987	4.064	702.8	569.2	227.1	209.0	9.3	4.6	S	S	6.06	4.58
	4.033[b]	4.063[b]	518.26[b]	502.77[b]	220.24[b]	214.23[b]	9.54[b]	4.05[b]				
Mn	3.945	4.025	682.1	550.0	241.6	217.8	−13.3	−8.5	U	U	5.66	4.15
Fe	3.927	4.010	543.1	428.7	299.3	263.4	−44.5	−29.9	U	U	6.07	4.64
Co	3.927	4.015	518.0	417.9	278.9	237.2	56.2	75.2	S	S	6.09	4.97
Ni	3.981	4.076	485.1	383.0	230.8	194.1	89.1	86.3	S	S	5.53	4.36
Cu	4.084	4.188	395.8	308.9	186.5	155.6	64.7	60.5	S	S	4.34	3.29
Zn	4.203	4.313	328.1	249.4	151.2	127.2	72.9	61.7	S	S	3.35	2.42

[a] Holec *et al* [23] (GGA).
[b] Brik *et al* [24] (LDA and GGA).
[c] See footnote 1 (Exp.)
[d] Kim *et al* [59] (Exp.)
[e] Meng and Eesley [30] (Exp.)

Table 3. Lattice constant (a), elastic constants (C_{11}, C_{12}, C_{44}), mechanical stability and cohesive energy per atom (E_{coh}) of the nitrides (MN) of 3d transition metals (M) in the cesium chloride structure. Stable phases are denoted as 'S' and unstable ones as 'U'.

	a (Å)		C_{11} (GPa)		C_{12} (GPa)		C_{44} (GPa)		Mechanical stability		E_{coh} (eV/atom)	
M	LDA	GGA	LDA	GGA	LDA	GGA	LDA	GGA	LDA	GGA	LDA	GGA
Sc	2.739	2.797	509.7	495.9	60.4	24.0	−120.3	−118.1	U	U	6.53	5.51
Ti	2.581	2.634	654.5	584.7	119.6	92.7	53.0	26.3	S	S	7.39	6.15
V	2.495	2.546	1023.5	915.5	48.2	19.0	180.3	140.4	S	S	7.01	5.61
Cr	2.452	2.503	969.5	819.0	111.2	93.1	40.0	−5.9	S	U	5.68	4.17
Mn	2.433	2.485	971.8	825.3	110.6	85.8	48.6	28.0	S	S	5.30	3.75
Fe	2.431	2.487	894.7	757.0	126.1	93.9	39.8	18.9	S	S	5.69	4.21
Co	2.454	2.515	600.5	483.9	210.3	173.4	30.8	4.7	S	S	5.57	4.42
Ni	2.489	2.551	576.3	482.7	170.4	131.5	−4.1	−6.8	U	U	5.03	3.87
Cu	2.552	2.619	391.4	320.7	180.8	140.8	10.5	4.5	S	S	3.94	2.90
Zn	2.639	2.710	257.7	205.4	166.8	134.6	−40.4	−37.6	U	U	2.82	1.94

The obtained a, C_{11}, C_{12} and C_{44} are shown in tables 1–3. Values from LDA and GGA are both listed. Comparison with other theoretical and experimental values for some rs-structured phases is also provided [23, 24, 30, 59][4] in table 2. Our computed values of a, C_{11}, C_{12} and C_{44} for rs-ScN, rs-TiN, rs-VN and rs-CrN agree very well with other theoretical [23, 24] and experimental results [30, 59] (see footnote 1). In figure 2, the primitive cell volumes (V) are shown, calculated by $V = a^3/4$ for zb and rs structures and $V = a^3$ for the cc structure. The trend of V across the row changes with the atomic radii of transition metals that first become smaller and then larger from column 3 to column 12 in the periodic table [60].

In order to be mechanically stable, crystals have to satisfy certain criteria. For cubic structures they are [61]

$$C_{11} - C_{12} > 0, \qquad C_{11} + 2C_{12} > 0, \qquad C_{11} > 0 \qquad \text{and} \qquad C_{44} > 0. \tag{6}$$

The mechanical stability of all structures explored is denoted as 'S' (stable) or 'U' (unstable). The cause of instability is always negative values of C_{44}, as is observed from tables 1–3.

[4] Powder diffraction files: ScN 00-045-0978, TiN 03-065-0565, VN 00-035-0768.

Table 4. Bulk modulus (B), polycrystalline shear modulus (G) and Young's modulus (E) of the nitrides (MN) of 3d transition metals (M). Unstable phases are denoted as 'U' without a numerical value. Zincblende structure is denoted as 'zb', rocksalt as 'rs' and cesium chloride as 'cc'.

	B (GPa)			G (GPa)			E (GPa)		
M	zb	rs	cc	zb	rs	cc	zb	rs	cc
Sc	140.7	197.1	181.3	45.4	155.2	U	122.9	368.8	U
Ti	200.2	280.2	256.7	83.8	188.7	77.5	220.6	462.4	211.3
V	234.1	318.0	317.9	47.6	152.6	228.5	133.7	394.7	553.0
Cr	254.7	329.1	335.0	U	41.2	U	U	118.7	U
Mn	267.5	328.5	332.3	44.8	U	104.5	127.4	U	283.8
Fe	267.9	318.5	314.9	80.4	U	87.2	219.3	U	239.4
Co	245.8	297.4	276.9	53.0	80.9	36.3	148.4	222.6	104.4
Ni	211.5	257.0	248.6	29.2	89.5	U	83.7	240.6	U
Cu	167.8	206.7	200.8	23.4	66.5	23.0	67.2	180.2	66.3
Zn	132.7	167.9	158.2	23.1	61.5	U	65.6	164.3	U

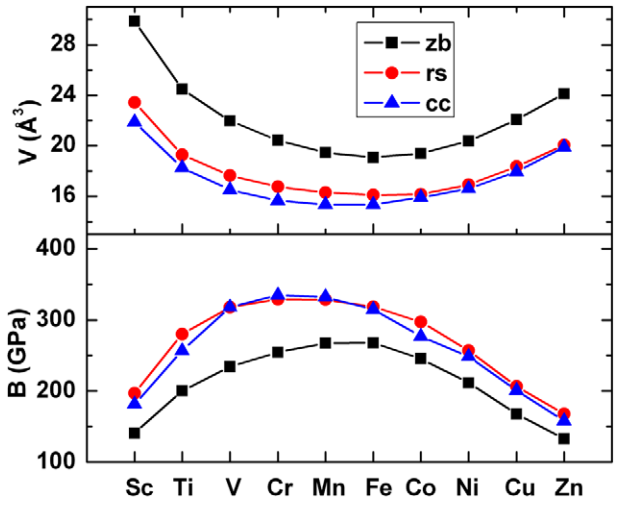

Figure 2. Computed equilibrium primitive cell volume (V) and bulk modulus (B) of the nitrides (MN) versus their corresponding 3d transition metals (M). The three structures are zincblende (zb, black square), rocksalt (rs, red circle) and cesium chloride (cc, blue triangle). The data in the two panels suggest anti-correlation of B with V.

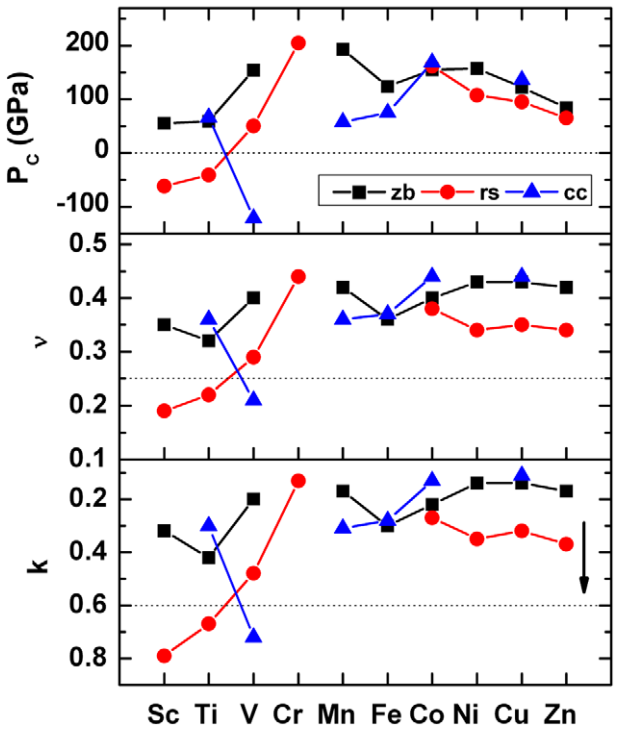

Figure 3. Cauchy's pressure (P_C), Poisson's ratio (ν) and Pugh's ratio (k) of the nitrides (MN) versus their corresponding 3d transition metals (M). The three structures are zincblende (zb, black square), rocksalt (rs, red circle) and cesium chloride (cc, blue triangle). Data have not been shown for mechanically unstable nitrides leading to breaks in the lines, which are only a guide to the eye. The y-axis in the lowest panel is inverted to show correlation between these quantities.

None of the other conditions in equation (6) are invalidated. Six nitrides are found to be unstable with both LDA and GGA. Additionally cc-CrN with GGA showed a slightly negative C_{44} value and hence was termed unstable. Note that the C_{44} of two phases, rs-CrN and cc-CuN, are positive but less than 10 GPa. These phases should be considered only marginally stable. The cc structure has the fewest stable compounds since 6 out of 10 are either unstable or only marginally stable.

Table 4 shows results for our computed values of B, G and E. Our data show that B is anti-correlated with V among TMNs of the same structure throughout the same row in the periodic table, shown in figure 2, consistent with earlier observations [19, 20, 22]. Specifically, values of B tend to peak in the middle of the rows at FeN for zb, CrN for rs and CrN for cc structures. This anti-correlation may be extended to comparison between different structures from our results. Thus, in figure 2, zb-structured phases generally have larger values of V compared with rs- and cc-structured ones of the same nitride composition and have smaller values of B.

Table 5 shows our values for P_C, ν and k. They are all good indicators of a material's brittle to ductile behavior. Combinations of conditions, such as $P_C \geq 0$, $\nu \geq 0.25$ and $k \leq 0.6$ [51, 62, 63], correlate with ductility. The bounding values in these inequalities, which determine their conditions, are marked by horizontal dotted lines in figure 3. Specifically, we observe that rs-ScN, rs-TiN and cc-VN are brittle while the other compounds have a ductile nature. Figure 3 further shows that high values of P_C and ν are accompanied by lower

Table 5. Cauchy's pressure (P_C), Poisson's ratio (ν) and Pugh's ratio (k) of the nitrides (MN) of 3d transition metals (M). Unstable phases are denoted as 'U' without a numerical value. Zincblende structure is denoted as 'zb', rocksalt as 'rs' and cesium chloride as 'cc'.

	P_C (GPa)			ν			k		
M	zb	rs	cc	zb	rs	cc	zb	rs	cc
Sc	55.1	−61.6	U	0.35	0.19	U	0.32	0.79	U
Ti	58.8	−40.9	66.4	0.32	0.22	0.36	0.42	0.67	0.30
V	154.1	50.3	−121.3	0.40	0.29	0.21	0.20	0.48	0.72
Cr	U	204.4	U	U	0.44	U	U	0.13	U
Mn	192.6	U	57.8	0.42	U	0.36	0.17	U	0.31
Fe	124.0	U	75.0	0.36	U	0.37	0.30	U	0.28
Co	154.6	162.0	168.7	0.40	0.38	0.44	0.22	0.27	0.13
Ni	157.2	107.7	U	0.43	0.34	U	0.14	0.35	U
Cu	122.4	95.1	136.3	0.43	0.35	0.44	0.14	0.32	0.11
Zn	84.1	65.5	U	0.42	0.34	U	0.17	0.37	U

Table 6. Vickers hardness H_{VA} from (9), Vickers hardness H_{VT} from (7) and Debye temperature (θ_D) of the nitrides (MN) of 3d transition metals (M). Unstable phases are denoted as 'U' without a numerical value. Zincblende structure is denoted as 'zb', rocksalt as 'rs' and cesium chloride as 'cc'.

	H_{VA} (GPa)			H_{VT} (GPa)			θ_D (K)		
M	zb	rs	cc	zb	rs	cc	zb	rs	cc
Sc	3.8	24.9	U	6.8	23.4	U	505.9	880.9	U
Ti	7.9	24.0	5.1	12.7	28.5	11.7	646.0	921.8	595.7
V	2.3	14.0	29.6	7.2	23.0	34.5	472.3	803.5	962.9
Cr	U	1.2	U	U	6.2	U	U	419.0	U
Mn	1.8	U	6.6	6.8	U	15.8	437.1	U	635.9
Fe	5.2	U	5.1	12.1	U	13.2	575.1	U	578.4
Co	2.7	4.7	1.2	8.0	12.2	5.5	460.5	550.1	370.6
Ni	1.1	6.7	U	4.4	13.5	U	346.7	581.5	U
Cu	0.9	5.0	0.7	3.5	10.0	3.5	304.7	492.7	291.9
Zn	1.2	5.4	U	3.5	9.3	U	303.2	473.8	U

values of k, where we note, with an arrow, that the k values have been plotted with an inverted axis.

Another property of interest is the Vickers hardness (H_V). There has been significant body of work on finding the connection between H_V and elastic properties [64–66]. These studies have shown that the elastic moduli G and B both appear to influence H_V. Teter [64] observed a linear correlation of H_V with G in 1998, and Chen *et al* [65] described it as

$$H_{VT} = 0.151G. \tag{7}$$

However, there have been exceptions to this formula, such as tungsten carbide (WC), which has a very large shear modulus (282 GPa) and a much smaller H_V (30 GPa) [62] compared with the predicted value (42.3 GPa) [65]. In the quest for a better formula, Chen *et al* [65] proposed a non-linear correlation,

$$H_{VC} = 2(k^2G)^{0.585} - 3, \tag{8}$$

taking not only G into consideration, but also k, which is conceptually related to plasticity. Their fitting of this form to experimentally observed hardness data achieved very good results for large values of H_V. For materials with small values of H_V this form produced negative values due to the '−3' term, as observed by Tian *et al* [66]. In our work, the same problem arose and we chose to use Tian *et al*'s correction,

$$H_{VA} = 0.92k^{1.137}G^{0.708}. \tag{9}$$

The results for hardness calculated from equations (7) and (9) are listed in table 6. Our value of H_{VA} for rs-TiN (24.0 GPa) is comparable with the experimental values using ultra high vacuum dc magnetron sputter deposition by Shin *et al* [31] (20.2 GPa), reactive magnetron sputtering by Helmersson *et al* [67] (22 GPa), chemical vapor deposition/physical vapor deposition by Musil [68] (21 GPa) and value provided by Holleck [8] (21 GPa). Our value of H_{VA} for rs-VN (14.0 GPa) is close to the experimental result with reactive magnetron sputtering by Helmersson *et al* [67] (16.2 GPa) and the value provided by Holleck [8] (15.6 GPa). Plots of G and H_{VA} are shown in figure 4, to illustrate their common trends. Comparing them with figure 3, we observe a clear correlation between the calculated H_{VA} and brittleness because of the dependence on k in (9). Three aforementioned brittle phases, rs-ScN, rs-TiN and cc-VN, demonstrate large H_{VA}, greater than 24 GPa, as well. The correlation with G is also obvious, although with a slight deviation for rs-ScN, having a small G but large H_{VA}. Values of H_{VT} are generally larger than values of H_{VA} except for rs-ScN mentioned above. Values of Debye temperature (θ_D) are also shown in table 6, where almost all values for θ_D are greater than 300 K with rs-structured phases generally showing higher values.

Debye temperature and hardness are both influenced by the nature of atomic bonding. Hence there may exist some connection between the two. Abrahams *et al* [69] replaced B with H_V in the formula $\theta_D = a \times B^{1/2}\rho^{-1/6}M^{-1/3}$ derived

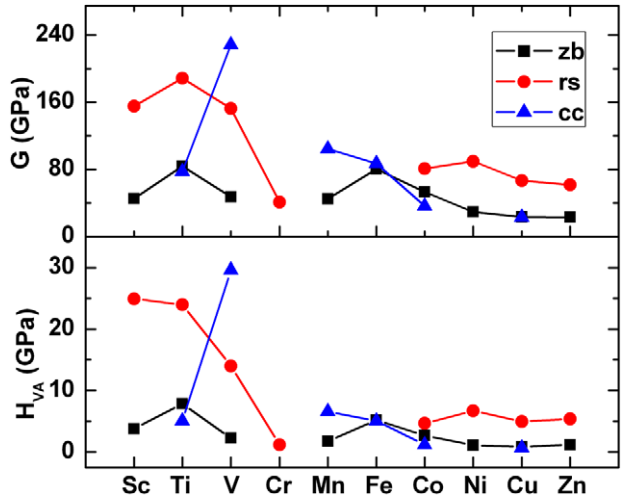

Figure 4. Polycrystalline shear modulus (G) and Vickers hardness (H_{VA}) from (9), of the nitrides (MN) versus their corresponding 3d transition metals (M). The three structures are zincblende (zb, black square), rocksalt (rs, red circle) and cesium chloride (cc, blue triangle). Data have not been shown for mechanically unstable nitrides, leading to breaks in lines, which are only a guide to the eye.

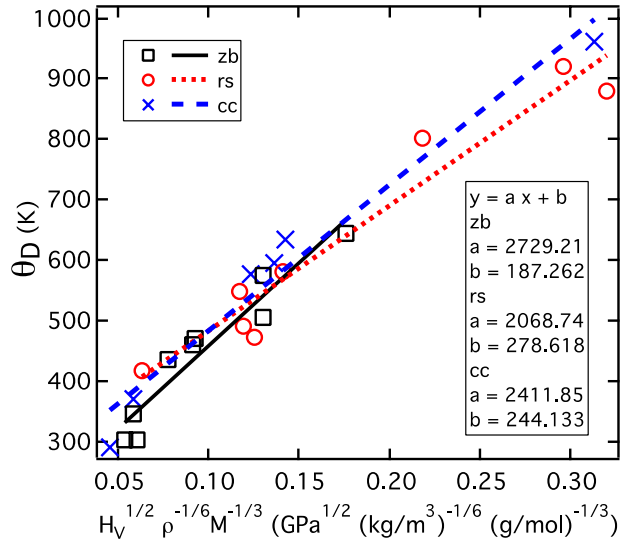

Figure 5. Debye temperature (θ_D) versus the formula containing hardness (H_V) as (10). The three structures are zincblende (zb, black open square), rocksalt (rs, red open circle) and cesium chloride (cc, blue ×). Symbols are data points that have been shown only for mechanically stable structures. The lines are linear fits to (10) for the three structures, respectively.

60 years ago by Madelung [70] and Einstein [71, 72] for the ease of experimentally measuring H_V. Deus [73] further added a constant to the formula and achieved better precision. Their formula is expressed as

$$\theta_D = a \times H_V^{1/2} \rho^{-1/6} M^{-1/3} + b, \qquad (10)$$

where a and b are linear fitting coefficients. A plot of this relationship, using H_{VA} values for H_V, along with the fitting parameters a and b, is displayed in figure 5. The correlation is notable but significantly better fits have been found in

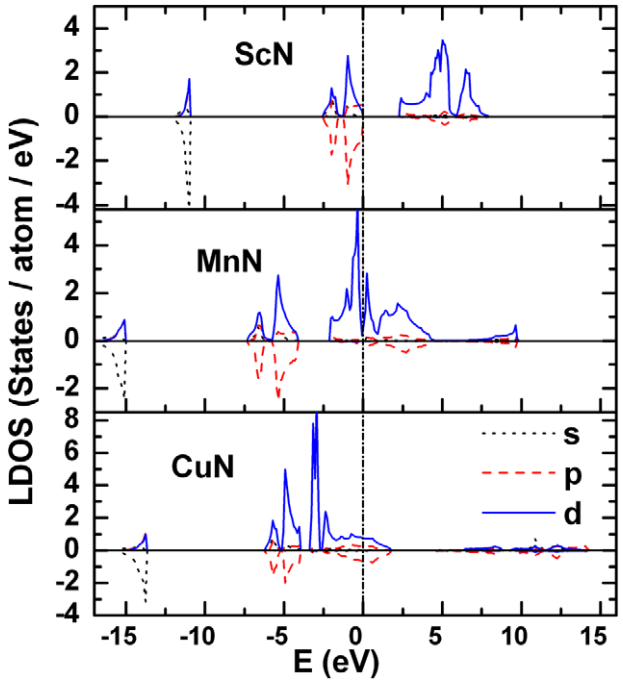

Figure 6. Local density of states (LDOS) of zincblende (zb) structured ScN, MnN and CuN. Nitrogen LDOS have been plotted as negative values for clarity. The most prominent peaks depict the hybridization of metal d orbitals with nitrogen p orbitals. Fermi energy is set to zero in each panel.

diamond-like semiconducting compounds by Deus [73] and in Ta_3B_4-structured early 3d, 4d, 5d transition metal borides by Miao *et al* [63]. Debye temperature can also be correlated with melting point (T_m) given by Lindemann [74] as $\theta_D = a \times T_m^{1/2} M^{-1/2} V^{-1/3}$. If a material has a large value of H_V, it will also have a large value of T_m. The combination of these two properties makes super-hard materials very promising candidates under high-temperature operations.

We obtained the plots of local or projected density of states (LDOS) for all 30 phases and selected some of them to demonstrate the gradual change through the 3d transition metal row. Except for zb-ScN and rs-ScN, all phases are metallic due to absence of electronic energy gaps around the Fermi energy (E_F). For each structure type the LDOS of three compound MN, with an atomic number increment of 4 for M, are plotted in each of figures 6 (zb), 7 (rs) and 8 (cc), respectively. Thus M stands for the elements Sc, Mn and Cu. In all three figures, we observe several trends. (i) The s states of N (N-s) are fairly deep below E_F and are hybridized with M-p and M-d states. (ii) The difference between E_F and the average energy of these states first increases with increasing atomic number of M and then decreases, opposite to the trend in the primitive cell volume and following the trend in B as seen in figure 2, indicating a relationship between the three. (iii) The N-p and M-d states are distributed over a large range of energies below and above E_F and are mutually hybridized. (iv) Both the N-p and M-d states show multiple peaks. (v) The M-d states tend to fall farther below E_F as we increase the atomic number of M along the 3d row, at least partially due to the increasing filling of the d-band. (vi) The d states also show

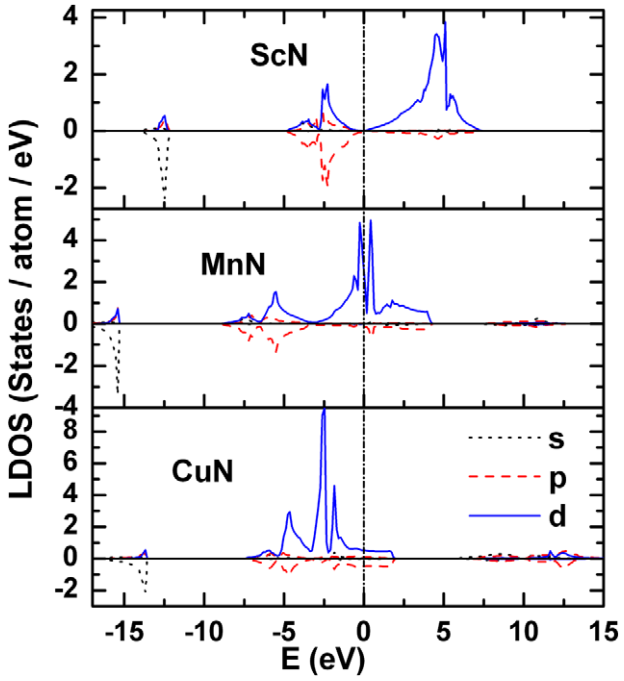

Figure 7. LDOS of rocksalt (rs) structured ScN, MnN and CuN. Nitrogen LDOS have been plotted as negative values for clarity. The most prominent peaks depict the hybridization of metal d orbitals with nitrogen p orbitals. Fermi energy is set to zero in each panel.

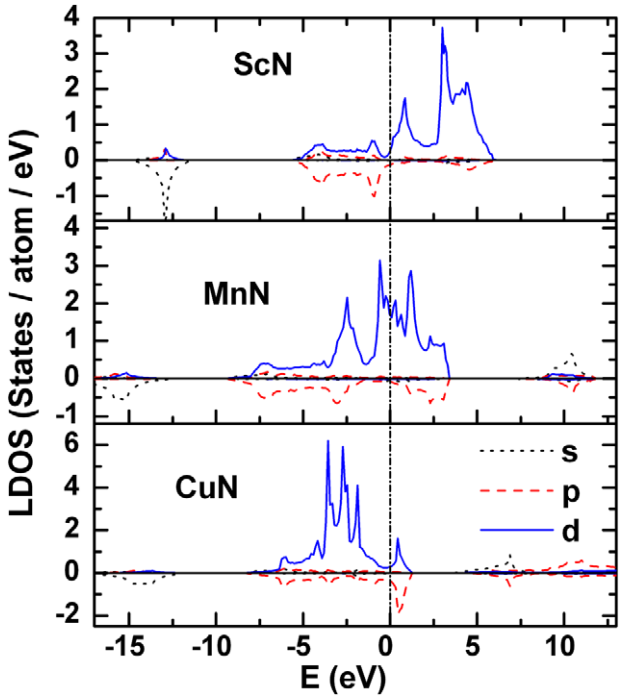

Figure 8. LDOS of cesium chloride (cc) structured ScN, MnN and CuN. Nitrogen LDOS have been plotted as negative values for clarity. The most prominent peaks depict the hybridization of metal d orbitals with nitrogen p orbitals. Fermi energy is set to zero in each panel.

narrower and higher peaks as opposed to the initially broader and lower ones as this d-band gets filled.

It has been observed for several materials that if the total density of states (TDOS) is high at E_F, the structure tends to be unstable, and vice versa [9, 21, 75]. In our work we have tested ten elements and three structures of each, rendering rich data to systematically analyze the correlation. In order to eliminate the imprecision caused by sharp changes in the TDOS from one specific energy value to the next, we integrated them over a window of -0.2 eV and 0.2 eV around E_F to achieve a more smoothly behaving quantity—the total number of electronic states in this window. This is plotted in figure 9 along with C_{44} from GGA, the decisive elastic constant of a structure's stability and hardness. Tests using the TDOS precisely at E_F show a trend that is not as obvious as the one rendered here, but still highly recognizable. The overall anti-correlation between the number of states in our window and C_{44} is suggestive, noting that the top panel in figure 9 has an inverted axis as shown by the arrow. It is fairly strong for the rs and zb structures but not so clear for the cc structure. We note here that for values of $C_{44} < 20$ GPa, the uncertainty in the numerical result is large due to the limitation of precision in this study. Many of the cc-structured compounds have low C_{44} values, making conclusions about anti-correlation less reliable.

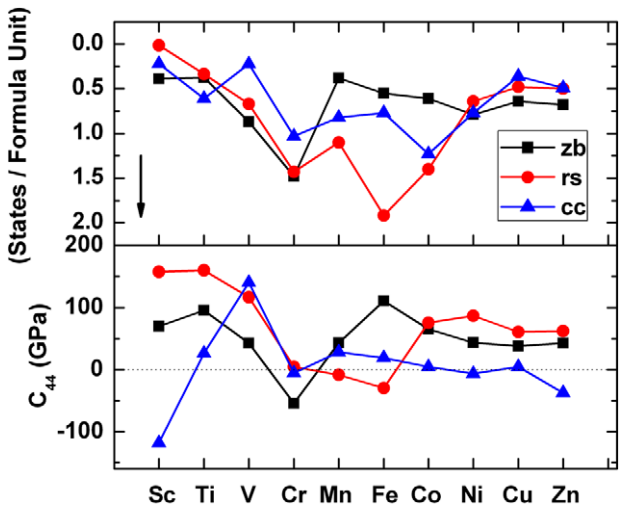

Figure 9. The number of electronic states per formula unit around E_F (from -0.2 eV to 0.2 eV) and elastic constant C_{44} of the nitrides (MN) versus their corresponding 3d transition metals (M). The three structures are zincblende (zb, black square), rocksalt (rs, red circle) and cesium chloride (cc, blue triangle). The y-axis in the upper panel is shown inverted to show correlation between these quantities. The data in the two panels suggests anti-correlation of C_{44} with the number of electronic states around E_F.

Our systematic set of computations allows us to make some comparisons in figures 2 and 4. Values for the compressibility, which is defined as $1/B$, correlate well with the primitive cell volume (V) in figure 2. Compressibility reflects the elastic properties under hydrostatic pressure that leads to no change of the bond angles. Hardness, on the other hand, deals with local plastic deformation, which is more related to shear distortion. We can easily see from figures 2 and 4 that the two quantities B and H_{VA} do not follow the same trend. However, H_{VA} is partially correlated with G, a shear

elastic quantity, and k, calculated by G/B, as pointed out earlier by Chen *et al* [65] and Tian *et al* [66].

Finally we point out some nuances in the computational precision of elastic constants. In order to get precise elastic constants, one should be careful while choosing the k-point sampling meshes and strain ratio. Although convergence below ± 1 meV is not strictly required for the lattice constant tests, it is critical for calculations of elastic constant C_{44}, because the energy difference between strained and unstrained cells is often smaller than 1 meV if the corresponding C_{44} falls below 20 GPa. For some tests giving small values of C_{44}, such as rs-CrN, cc-CoN and cc-CuN, we used meshes up to $26 \times 26 \times 26$ and a larger strain ratio set for C_{44} to keep the aforementioned energy difference large enough to stand out from the precision uncertainty.

4. Conclusion

In summary, we performed first-principles calculations with density functional theory on three cubic stoichiometric (1:1) structures, zincblende, rocksalt and cesium chloride, of ten nitride phases each formed by 3d transition metals. We observed the anti-correlation of bulk modulus, a good indicator of bond strength, with the primitive cell volume, which is closely associated with bond length. Among all 30 phases, a good degree of Vickers hardness, higher than 24 GPa, was observed in rs-ScN, rs-TiN and cc-VN. Vickers hardness was related to a material's shear modulus and brittle to ductile behavior, characterized by Cauchy's pressure, Poisson's ratio and Pugh's ratio, and was used to estimate the Debye temperature, following earlier work [69–73]. Furthermore, with the rich data gathered from these tests, trends in the density of states were systematically analyzed. In addition, we showed the anti-correlation of the elastic constant C_{44}, which indicates stability and hardness, with the number of electronic states around the Fermi energy.

Acknowledgments

The authors thank the Ohio Supercomputer Center (OSC) for the computing resources. We thank the National Science Foundation CMMI 1234777, CNS 0855134, DMR CMMI 0928440 and CMMI 0933069 for funding this work. We thank an anonymous referee for motivating us to add figure 1 and its discussion.

References

[1] Jhi S H, Ihm J, Louie S G and Cohen M L 1999 *Nature* **399** 132
[2] Jhi S H, Louie S G, Cohen M L and Ihm J 2001 *Phys. Rev. Lett.* **86** 3348
[3] Jhi S H, Louie S G, Cohen M L and Morris J W 2001 *Phys. Rev. Lett.* **87** 075503
[4] Liu A Y and Cohen M L 1989 *Science* **245** 841
[5] Chen X J *et al* 2005 *Proc. Natl Acad. Sci. USA* **102** 3198
[6] Kodambaka S, Khare S V, Petrov I and Greene J E 2006 *Surf. Sci. Rep.* **60** 55
[7] Kodambaka S, Khare S V, Petrova V, Johnson D D, Petrov I and Greene J E 2003 *Phys. Rev.* B **67** 035409
[8] Holleck H 1986 *J. Vac. Sci. Technol.* A **4** 2661
[9] Montoya J A, Hernandez A D, Sanloup C, Gregoryanz E and Scandolo S 2007 *Appl. Phys. Lett.* **90** 011909
[10] Young A F, Sanloup C, Gregoryanz E, Scandolo S, Hemley R J and Mao H K 2006 *Phys. Rev. Lett.* **96** 155501
[11] Crowhurst J C, Goncharov A F, Sadigh B, Evans C L, Morrall P G, Ferreira J L and Nelson A J 2006 *Science* **311** 1275
[12] Gregoryanz E, Sanloup C, Somayazulu M, Badro J, Fiquet G, Mao H K and Hemley R J 2004 *Nature Mater.* **3** 294
[13] Butenko Y V, Alves L, Brieva A C, Yang J, Krishnamurthy S and Siller L 2006 *Chem. Phys. Lett.* **430** 89
[14] Siller L, Peltekis N, Krishnamurthy S, Chao Y, Bull S J and Hunt M R C 2005 *Appl. Phys. Lett.* **86** 221912
[15] Krishnamurthy S, Montalti M, Wardle M G, Shaw M J, Briddon P R, Svensson K, Hunt M R C and Siller L 2004 *Phys. Rev.* B **70** 045414
[16] Liang Y C, Li C, Guo W L and Zhang W Q 2009 *Phys. Rev.* B **79** 024111
[17] Zhao W J, Bin Xu H and Wang Y X 2009 *Phys. Status Solidi RRL* **3** 272
[18] Patil S K R, Khare S V, Tuttle B R, Bording J K and Kodambaka S 2006 *Phys. Rev.* B **73** 104118
[19] Zhao E J, Wang J P, Meng J and Wu Z J 2010 *Comput. Mater. Sci.* **47** 1064
[20] Zhao E J and Wu Z J 2008 *J. Solid State Chem.* **181** 2814
[21] Patil S K R, Mangale N S, Khare S V and Marsillac S 2008 *Thin Solid Films* **517** 824
[22] Chen W and Jiang J Z 2010 *J. Alloys Compunds* **499** 243
[23] Holec D, Friak M, Neugebauer J and Mayrhofer P H 2012 *Phys. Rev.* B **85** 064101
[24] Brik M G and Ma C G 2012 *Comput. Mater. Sci.* **51** 380
[25] Zaoui A, Kacimi S, Bouhafs B and Roula A 2005 *Physica* B **358** 63
[26] Eck B, Dronskowski R, Takahashi M and Kikkawa S 1999 *J. Mater. Chem.* **9** 1527
[27] Häglund J, Grimvall G, Jarlborg T and Guillermet A F 1991 *Phys. Rev.* B **43** 14400
[28] Chen H H, Peng F, Mao H K, Shen G Y, Liermann H P, Li Z O and Shu J F 2010 *J. Appl. Phys.* **107** 113503
[29] Liu K, Zhou X L, Chen H H and Lu L Y 2012 *Physica* B **407** 3617
[30] Meng W J and Eesley G L 1995 *Thin Solid Films* **271** 108
[31] Shin C S, Gall D, Hellgren N, Patscheider J, Petrov I and Greene J E 2003 *J. Appl. Phys.* **93** 6025
[32] Shebanova O, Soignard E and McMillan P F 2006 *High Press. Res.* **26** 87
[33] Dzivenko D, Zerr A, Guignot N, Mezouar M and Riedel R 2010 *Europhys. Lett.* **92** 66001
[34] Wang Y C, Yao T K, Li H, Lian J, Li J H, Li Z P, Zhang J W and Gou H Y 2012 *Comput. Mater. Sci.* **56** 116
[35] Hugosson H W, Jansson U, Johansson B and Eriksson O 2001 *Science* **293** 2434
[36] de Paiva R, Nogueira R A and Alves J L A 2007 *Phys. Rev.* B **75** 085105
[37] Korir K K, Amolo G O, Makau N W and Joubert D P 2011 *Diamond Relat. Mater.* **20** 157
[38] Srivastava A, Chauhan M and Singh R K 2011 *Phys. Status Solidi* b **248** 2793
[39] Kohn W and Sham L J 1965 *Phys. Rev.* **140** 1133
[40] Kresse G and Furthmuller J 1996 *Phys. Rev.* B **54** 11169
[41] Kresse G and Furthmuller J 1996 *Comput. Mater. Sci.* **6** 15
[42] Kresse G and Hafner J 1993 *Phys. Rev.* B **48** 13115
[43] Vanderbilt D 1990 *Phys. Rev.* B **41** 7892
[44] Kresse G and Hafner J 1994 *J. Phys.: Condens. Matter* **6** 8245
[45] Ceperley D M and Alder B J 1980 *Phys. Rev. Lett.* **45** 566

[46] Perdew J P, Chevary J A, Vosko S H, Jackson K A, Pederson M R, Singh D J and Fiolhais C 1992 *Phys. Rev.* B **46** 6671
[47] Stampfl C, Mannstadt W, Asahi R and Freeman A J 2001 *Phys. Rev.* B **63** 155106
[48] Juan Y M and Kaxiras E 1993 *Phys. Rev.* B **48** 14944
[49] Ateser E, Ozisik H, Colakoglu K and Deligoz E 2011 *Comput. Mater. Sci.* **50** 3208
[50] Fan C Z, Zeng S Y, Li L X, Zhan Z J, Liu R P, Wang W K, Zhang P and Yao Y G 2006 *Phys. Rev.* B **74** 125118
[51] Ivanovskii A L 2012 *Prog. Mater. Sci.* **57** 184
[52] Lopuszynski M and Majewski J A 2007 *Phys. Rev.* B **76** 045202
[53] Wu Z and Meng J 2008 *Comput. Mater. Sci.* **43** 495
[54] Yang Y, Lu H, Yu C and Chen J M 2009 *J. Alloys Compunds* **485** 542
[55] Monkhorst H J and Pack J D 1976 *Phys. Rev.* B **13** 5188
[56] Murnaghan F D 1944 *Proc. Natl Acad. Sci. USA* **30** 244
[57] Fu H Z, Li D H, Peng F, Gao T and Cheng X L 2008 *Comput. Mater. Sci.* **44** 774
[58] Blöchl P E, Jepsen O and Andersen O K 1994 *Phys. Rev.* B **49** 16223
[59] Kim J O, Achenbach J D, Mirkarimi P B, Shinn M and Barnett S A 1992 *J. Appl. Phys.* **72** 1805
[60] Pearson W B 1972 *The Crystal Chemistry and Physics of Metals and Alloys* (New York: Wiley) p 151 (Table 4-4)
[61] Wallace D C 1972 *Thermodynamics of Crystals* (New York: Wiley) chapter 1
[62] Haines J, Leger J M and Bocquillon G 2001 *Annu. Rev. Mater. Sci.* **31** 1
[63] Miao N H, Sa B S, Zhou J A and Sun Z M 2011 *Comput. Mater. Sci.* **50** 1559
[64] Teter D M 1998 *MRS Bull.* **23** 22
[65] Chen X Q, Niu H Y, Li D Z and Li Y Y 2011 *Intermetallics* **19** 1275
[66] Tian Y, Xu B and Zhao Z 2012 *Int. J. Refract. Met. Hard Mater.* **33** 93
[67] Helmersson U, Todorova S, Barnett S A, Sundgren J E, Markert L C and Greene J E 1987 *J. Appl. Phys.* **62** 481
[68] Musil J 2000 *Surf. Coat. Technol.* **125** 322
[69] Abrahams S C and Hsu F S L 1975 *J. Chem. Phys.* **63** 1162
[70] Madelung E 1910 *Phys. Z.* **11** 898
[71] Einstein A 1911 *Ann. Phys., Lpz.* **34** 170
Einstein A 1911 *Ann. Phys., Lpz.* **34** 590
[72] Einstein A 1911 *Ann. Phys., Lpz.* **35** 679
[73] Deus P and Schneider H A 1983 *Cryst. Res. Technol.* **18** 491
[74] Lindemann F 1910 *Phys. Z.* **11** 609
[75] Wang Y X, Arai M and Sasaki T 2007 *Appl. Phys. Lett.* **90** 061922